J Mater Sci (2007) 42:624–632
DOI 10.1007/s10853-006-1154-9

The aqueous solution-gel synthesis of perovskite $Pb(Zr_{1-x},Ti_x)O_3$ (PZT)

K. Van Werde · G. Vanhoyland · D. Mondelaers · H. Den Rul · M. K. Van Bael · J. Mullens · L. C. Van Poucke

Received: 27 July 2004 / Accepted: 18 November 2005 / Published online: 7 December 2006

Abstract Starting from a novel water-based Zr(IV)-peroxo-citrato solution, an entirely aqueous solution-gel synthesis of $Pb(Zr_{0.53},Ti_{0.47})O_3$ (PZT) was carried out. Because of the tendency of Zr^{4+}-ions to hydrolyze and condensate extensively in water, the Zr^{4+}-ions had to be chemically modified by reaction with hydrogen peroxide and citric acid in a two-step precursor synthesis. A transparent amorphous PZT gel precursor was obtained by evaporating the solvent (water). This resulted in a network of cross-linked ammonium-carboxylate bonds that holds Zr(IV)-peroxo-citrato, Ti(IV)-peroxo-citrato and Pb(II)-citrate complexes. By combining complementary thermal analysis techniques such as HT-DRIFT (high-temperature diffuse reflectance Fourier-transform infrared spectroscopy), TGA-MS (thermogravimetrical analysis online coupled to mass spectrometry) and DTA (differential thermal analysis) insight in the decomposition mechanism of the PZT gel was gained. Three major regions could be distinguished; consecutively the non-coordinative matrix surrounding the metal ion complexes, the precursor complexes and the remaining organic matrix are being decomposed. The phase formation of crystalline perovskite PZT was investigated in situ by means of HT-XRD (high-temperature X-ray diffraction). It shows that sublimation of PbO leads to the phase segregation of a Zr-rich PZT phase when a stoichiometric PZT precursor is used. Single phase perovskite PZT however can be obtained at low temperature (~610 °C) when a 16 % lead excess is applied.

K. Van Werde · G. Vanhoyland · D. Mondelaers · H. Den Rul · M. K. Van Bael · J. Mullens (✉) · L. C. Van Poucke
Laboratory of Inorganic and Physical Chemistry, IMO, Limburgs Universitair Centrum, Diepenbeek B-3590, Belgium
e-mail: jules.mullens@uhasselt.be

Introduction

Recently several attempts to prepare a variety of functional (electronic) ceramics, that use *water as a solvent* in their precursor gel synthesis, were explored successfully [1–13]. Like any other chemical precursor route the *Aqueous Solution-Gel method* meets the demands for a vast homogeneity in the precursor gel and the desired multimetal oxide, profound compositional and chemical control of synthesis parameters, low phase formation temperatures, short thermal treatments (favorable thermal budget) and suitable conditions for covering or making various shapes of objects, such as thin films, fibers or wires. In addition, the aqueous solution-gel method offers some further advantages. Unlike several metal alkoxide precursor solutions, these aqueous precursor solutions are insensitive to ambient moisture. Therefore, an inert atmosphere to store and handle precursor solutions (the use of a nitrogen flushed glove boxe) and costly starting products can be avoided [12]. Because water is applied as a solvent, instead of the often used teratogenic ether alcohols (e.g. methoxyethanol), the aqueous solution-gel synthesis can be considered healthier, safer and environmentally friendlier. Moreover it has recently been shown that the aqueous chemical solution deposition (CSD) of thin precursor films on top of an adequate substrate can lead to

functional (conducting or ferroelectric) thin ceramic layers [9–12, 14].

In this report the aqueous solution-gel synthesis of perovskite $Pb(Zr_{1-x},Ti_x)O_3$ (PZT) is discussed. Because of its versatile ferroelectric, piezoelectric, pyroelectric, electro-optic and other functional properties, PZT has become one of the most widely investigated and important perovskite-type multimetal oxides over the past 10 years [14–16] (therefore it is appealing to explore the viability of the proposed aqueous solution-gel synthesis for this ceramic). This study not only is interesting from a materials research point of view, but might also offer deeper insight in the aqueous solution gel chemistry of high valent cations like Zr^{4+} and Ti^{4+} (that are insoluble as such in aqueous media) [17]. Moreover the thermal decomposition of their (ammonium peroxo-citrato-) gels and the phase formation of perovskite PZT from these precursors needs investigation, because it has been shown that both the chemistry and the thermal decomposition of the PZT precursor have significant influence on the properties of the crystallized end product [18–19].

Experimental

Materials and reagents

For the gel synthesis the following materials and reagents were used: citric acid (Aldrich, 99 %, $C(OH)(COOH)(CH_2COOH)_2$), ammonia (UCB, p.a. NH_3 ca 25 % in H_2O), titanium(IV)-isopropoxide (Acros, 98$^+$%, $Ti(OPr^i)_4$), zirconium(IV)-n-propanolate (Fluka, ~70% in propanol, $Zr(OPr^n)_4$), Lead(II)-acetate trihydrate (Merck, p.a. $Pb(OOCCH_3)_2.3H_2O$) and hydrogen peroxide (Acros Organics, p.a. 35 % H_2O_2 solution in H_2O, stabilized).

Methods and apparatus

Metal ion concentrations in solution were determined with ICP-AES (Inductively Coupled Plasma – Atomic Emission Spectroscopy) on a Perkin-Elmer Optima 3000 DV.

The thermal decomposition of the PZT-precursor gel was studied by means of thermogravimetrical analysis (TGA) (TA instruments TGA 951-2000 apparatus) on-line coupled to a quadrupole mass spectrometer (MS) (Model Thermolab of VG Fisons Instruments, using a flexible heated silica lined steel capillary and a molecular leak). The exact coupling for this evolved gas analysis technique is described elsewhere (TGA-EGA) [20]. In TGA-MS the gaseous molecules are fragmented (by ionization) prior to detection (of the resulting ions). This hyphenated technique thereby allows qualitative analysis of the gasses emitted during the thermal decomposition of the gels. In TGA-MS an ionization energy of 20 eV was used (in stead of the typical 70 eV) in order to distinguish NH_3^+ from OH^+ at m/q 17, since a low ionization energy inhibits the creation of OH^+-ions [6, 7, 21]. In all TGA-MS experiments a dry air-like mixture of O_2 and N_2 (provided by Air Liquide) was used as a carrier gas (with a flow rate of 100 ml min^{-1}). Every experiment was carried out at a heating rate of 10 °C min^{-1}.

The chemical changes occurring in the solid phase of the decomposing gel [5–7] can be studied by means of in situ high temperature – diffuse reflection Fourier transform infrared spectroscopy (HT-DRIFT), which identifies solid intermediate decomposition products by their IR-active groups. An FTIR apparatus (Bruker IFS 66 spectrometer) equipped with a high temperature – high pressure chamber with parabolic ZnSe windows (Spectratech Inc. (0030-011)) was used (a resolution of 4 cm^{-1} was selected for a DTGS-detector). The in situ HT-DRIFT investigations were carried out on 2 w/w% diluted precursor gels in ZnSe or KBr at a heating rate of 10 °C min^{-1} under a continuous carrier gas flow of 100 ml min^{-1}. The heating was controlled with a Eurotherm digital temperature controller (model 808). In dry air a temperature of about 440 °C could not be exceeded, since the HT-DRIFT-compartment will oxidize at higher temperatures.

In order to investigate the exo- and endothermic nature of the occurring decomposition processes, differential thermal analysis (DTA) was carried out for the PZT precursor. For the DTA experiment (on a DTA 1600–2000 from TA instruments) a heating rate of 10 °C min^{-1} and a gas flow of 100 ml min^{-1} were selected.

Phase formation of crystalline PZT was studied in situ by means of high temperature X-ray diffraction (HT-XRD) (Siemens D-5000, Cu-K_α). For this study the equipment was operated in the hot-stage mode. The configuration consisted of a Göbel mirror ($K_{\alpha 1+2}$, Huber), a high temperature device with a Pt heating rod (Anton Paar, HTK 10) and a position sensitive detector (Braun). The contributions of the Pt rod at 39.76°, 46.24° and 67.45° 2θ should be neglected when analyzing the spectra. For the HT-XRD experiments a heating rate of 10 °C min^{-1} in static dry air was employed.

Aqueous solution-gel synthesis

Synthesis of a Zr^{4+}-peroxo-citrato precursor solution

A first step in the aqueous solution-gel synthesis of a multimetal oxide involves the preparation of a stable, homogeneous precursor solution containing all metal ions in a pH region that is suitable for gel formation [4, 6]. However, the aqueous chemistry of soluble Zr^{4+} (and Ti^{4+}) is limited to a very acidic environment (pH < 1) [17].

Because of their high valence and their high electronegativity these cations hydrolyze rapidly and subsequently condensate extensively (the latter by olation and successive oxolation), inevitably resulting in the formation of (insoluble) hydrated oxides at lower acidities (higher pH) [17, 22, 23]. Therefore trying to introduce these cations as such in an aqueous multimetal ion system at milder pH would ruin the so-desired homogeneous mixing of cations on an atomic level.

It has been shown nonetheless that high-valency metal ions can be introduced in water at moderate acidity by chemically modifying the cation. That is, by coordinating the metal ion to tailor-made ligands, one is able to reduce the overall tendency to hydrolyze and condensate [24, 25]. For Ti^{4+}, Nb^{5+} and Ta^{5+} this was already achieved by the syntheses of water soluble metal-peroxo-citrato complexes, wherein the peroxide- and citrate ligands (CIT) play a crucial role [1–6, 12, 13, 25]. In this study a similar synthesis of a new Zr(IV)-peroxo-citrato precursor solution was adopted. This precursor will be introduced in the aqueous solution-gel preparation of PZT.

In essence this synthesis method resembles the one of the Ti(IV)-peroxo-citrato precursor [4–6], although some major differences will be discussed further on. Figure 1 shows that in a first step of the precursor synthesis zirconium is hydrolyzed by adding Zr(IV)-propanolate to water under rapid stirring. In this way a hydrated, fresh zirconium(IV)-oxide precipitate is obtained. After repetitive, thorough washing with water and filtration over a 0.1 μm filter, the precipitate is mixed with an aqueous solution of citric acid and hydrogen peroxide in order to dissolve the oxide in acidic environment. One obtains a clear, intense yellow colored precursor solution after refluxing the aqueous mixture at 120 °C for 2 hours (referred to as precursor phase 1 in Fig. 1).

The pH of the solution is then increased up to 7.5 by the addition of ammonia. By adding ammonia not only most of the carboxylate groups of citric acid become deprotonated (pK_{A3} of citric acid is 6.39), favoring the desired carboxylato-coordination [7] of the Zr(IV)-ions, but also the decomposition of the excess H_2O_2 is thereby promoted [2,3]. For the latter reason the precursor solution is refluxed for another two hours at 120 °C. The stable and clear yellow solution obtained after this treatment (referred to as precursor phase 2 in Fig. 1), is called the Zr(IV)-peroxo-citrato precursor solution.

The resulting precursor solution is assumed to contain Zr(IV)-peroxo-citrato complexes resembling the binuclear metal-peroxo-citrato complexes of Nb^{5+} [2,25], Ta^{5+} [13] and V^{5+} [26]. Herein coordination of a side-on peroxo-group (O_2 > M) and respectively the α-hydroxy-group and carboxylato-groups of the chelating citrate ion not only reduce the overall charge of the metal ion, but also shield the ion from surrounding water molecules, thereby preventing fast hydrolysis and extensive condensation/precipitation in water.

In contrast with the synthesis of the Ti(IV)-peroxo-citrato precursor solution [4–6] a CIT:Zr and H_2O_2:Zr ratio of at least 4:1 and 13:1 are required in order to dissolve all hydrated ZrO_2 in precursor phase 1. For titanium these constraints were about 2:1 for both ratio's. Moreover, for Zr(IV) the mixture has to be refluxed at 120 °C instead of the customary 60 ° to 70 °C for other high valent metal ion precursors [3–6, 13]. Both these differences might be due to the extensive polymerization degree of hydrated amorphous ZrO_2, that originates from hydrolyzed and condensated tetranuclear $Zr_4(OH)_8(OH_2)_{16}^{8+}$-species [17]. However, it has been shown that the presence of peroxide molecules promotes the breaking of the *ol*-bonds (2 μ_2-OH) in tetranuclear complexes of zirconium [27]. Therefore it is assumed that their occurrence, as well as the mild acidic conditions and the high reflux temperature in precursor phase 1, enable the complete depolymerization (and dissolving) of the hydrated oxide.

Synthesis of the PZT precursor gel

For the synthesis of the PZT precursor gel an aqueous Zr(IV)-peroxo-citrato solution of about 0.2 mol l^{-1} was synthesized according to the above procedure. In order to obtain a fast, yet flexible synthesis route, the applied CIT:Zr and H_2O_2:Zr ratios were increased to 6:1 and 20:1 (the hydrated oxide dissolves faster). As seen in Fig. 1 an aqueous Ti(IV)-peroxo-citrato solution of about 0.2 mol l^{-1}, was added stoichiometrically after precise determination of both metal ion concentrations (by means of ICP-AES). To obtain a morphotropic phase boundary composition of PZT a Zr:Ti ratio of

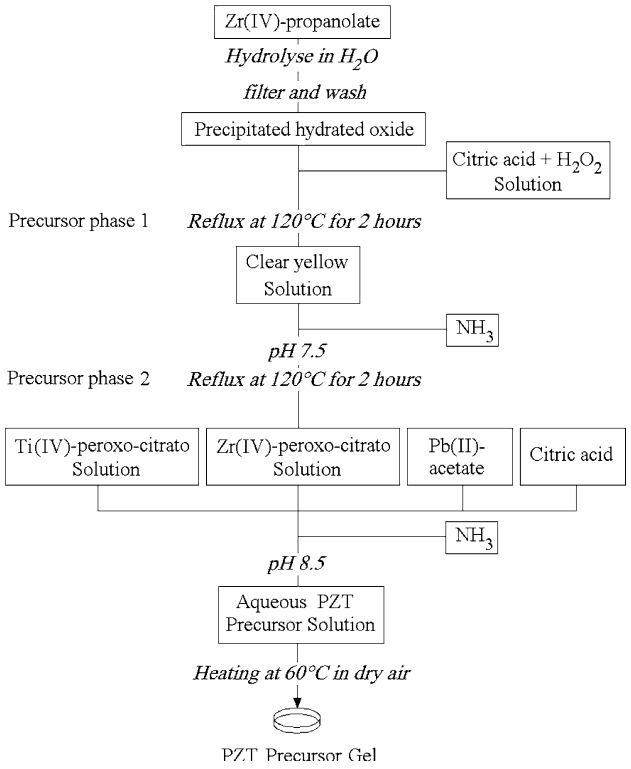

Fig. 1 Flow chart of the synthesis of the Zr(IV)-peroxo-citrato solution and the PZT gel

0.53:0.47 was selected [28]. After that a well chosen amount of Pb(II)-acetate (vide infra) and a small quantity of extra citric acid were added at pH 8.5. The addition of the extra citric acid and the lower acidity guarantee the complete dissolving of Pb^{2+} in the presence of citrate ions in water [1, 4].

The PZT precursor solution thus obtained contains an overall citrate to metal ratio, CIT:M_{total}, of 2:1. This amount of ligand is considerably lower than for other chemical synthesis routes, e.g. the Pechini-route [24], thereby strongly reducing the amount of carbon that has to be removed again in the precursor pyrolysis stage. The exact ratios of ligand and individual metal ions in the PZT precursor solution are summarized in Table 1.

The PZT precursor solution was then poured out in a Petri-vessel and the solvent (water) was subsequently evaporated in an air-flushed oven at 60 °C in order to allow gelation. The resulting dry ammonium peroxo-citrato PZT gel has a yellow color, is transparent,

Table 1 The exact ratios of citric acid and the individual metal ions in both PZT precursor solutions

CIT	Pb^{2+}	Zr^{4+}	Ti^{4+}	Lead excess
4.12	1.00	0.53	0.47	0%
4.32	1.16	0.53	0.47	16%

shows no precipitation and is amorphous, as shown by the absence of diffraction peaks in the XRD pattern at room temperature (in Fig. 5).

Not only the increase of concentration and its consequent high viscosity cause the precursor solution to form a homogeneous gel. Also several types of intermolecular cross-links, such as intermolecular ammonium-carboxylate interactions, hydrogen bonds and probably metal-carboxylate bonds contribute to the gel formation as well [1,4]. The DRIFT-spectrum of the PZT gel at 25 °C in Fig. 3 indicates clearly the interaction between NH_4^+-ions and carboxylate groups: the typical $\nu_{as}(COO^-/NH_4^+)$ and $\nu_{sym}(COO^-/NH_4^+)$ stretches (around 1595 and 1400 cm^{-1} respectively) and the ν(OH) and ν(NH) stretches involved in hydrogen bonding (in a broad band in between 3400 and 2500 cm^{-1}) are undoubtedly present [7].

It is believed that particularly the cross-linking of intermolecular ammonium-carboxylate interactions leads to the formation and the stability of the gel since a change of base from NH_3 to tetramethyl-ammonium-hydroxide (TMAH) during the synthesis (see Fig. 1) does not lead to gel formation. The larger conjugated acid of TMAH, the tetramethyl ammonium ion, contains no hydrogens directly bonded to an electro-negative element, and therefore can not form a H-bond with a carboxylato group, whereas NH_4^+ is able to do so. Therefore it is our believe that the presence of NH_4^+-ions, which serve as bridging cross-links between carboxylates and/or carboxylato-complexes, plays a crucial role in the formation of a three-dimensional network wherein all metal ions are distributed homogeneously [1,4].

The DRIFT spectrum at room temperature in Fig. 3 shows the existence of side-on bonded peroxo-groups ($\nu_1(M < O_2)$) [29] absorbing at 855 cm^{-1}. This absorption can not be attributed to the presence of non-coordinated H_2O_2, since the latter absorbs at 877 cm^{-1} [2]. For this reason it is believed that the excess H_2O_2 was completely decomposed during precursor synthesis (precursor phase 2).

The presence of the α-hydroxy-group (of the citrate ligand) coordinated to the metal ion is confirmed as well, given that the ν(C-O) stretch around 1090 cm^{-1} clearly differs from the ν(C-OH) stretch of a pure (metal ion free) ammonium citrate gel, (as described elsewhere [7]). Both the $\nu_1(M < O_2)$ stretch and the altered ν(C-O) prove the existence of metal-peroxo-citrato complexes in the gel.

In order to study the influence of the total amount of lead on the phase formation of PZT, a second precursor solution and gel, with a 16% excess of Pb^{2+} was synthesized following the same procedure.

Thermal decomposition of the PZT-gel

Since both the chemistry and the thermal decomposition behavior of the PZT precursor have significant influence on the phase formation and the properties of the crystallized end product [18, 19, 30, 31] it is of importance to characterize the chemical structures and the transformations that occur during the thermal treatment of the amorphous precursor. For the synthesized ammonium (peroxo-) citrate precursor it is therefore valuable to gather information about chemical and structural changes of the ammonium carboxylate network and the ammonium carboxylato-complexes by a set of (complementary) thermal analysis techniques [5–7].

TGA and DTA

The TGA, DTG (differential thermogram) and DTA profiles in Fig. 2 show that the decomposition of the PZT-precursor gel in dry air (at a heating rate of 10 °C min^{-1} and a gas flow of 100 ml min^{-1}) can be divided in three major temperature regions, typical for aqueous ammonium citrate precursor gels [6, 7].

In a first temperature region (T < 270 °C), corresponding with a weight loss of about 37%, several endothermal processes occur. The second temperature region of the decomposition (270 °C < T < 420 °C), features endothermal as well as exothermal disintegration steps and amounts for a weight loss of about 16 %. In the final region (420 °C < T < 520 °C), a very abrupt, highly exothermal reaction results in a sudden large weight loss of about 19 %. According to the DTG this decomposition is the fastest at 435 °C, after which it progresses slowly until 520 °C. From 520 °C on the absolute mass of the investigated sample remains constant *at first sight* and all organics are considered to be pyrolysed.

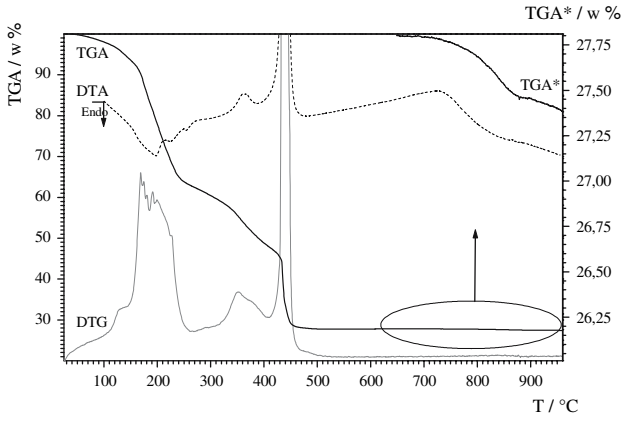

Fig. 2 Thermogravimetrical and differential thermal analysis for the PZT precursor gel in dry air at 10 °C min^{-1} [TGA (bold), DTG (grey), DTA (dashed)]. The upper right corner shows the enlarged thermogram [TGA^* (bold)]

Above 640 °C however an additional endothermal small weight loss is detected, indicated by the DTA-curve and the enlarged thermogram (in the upper right corner) of Fig. 2.

The latter phenomenon will be considered when discussing the phase formation of PZT. First of all the thermal decomposition during each of the earlier mentioned temperature regions will be discussed in more detail by means of the TGA-MS and HT-DRIFT results.

TGA-MS and HT-DRIFT

In the first temperature region (T < 270 °C) the direct coordination of the metal ions does not alter. As is typical for aqueous ammonium citrate precursor gels only the surrounding matrix of the metal ion complexes decomposes [6, 7]. The following endothermal processes are occurring: further drying of the sample; decomposition of non-coordinated ammonium carboxylate groups into carboxylic acids and evolving NH_3; decomposition of ammonium acetate yielding gaseous acetic acid and evolving NH_3; dehydroxylation of the α-hydroxy-carboxylates and α-hydroxy-carboxylic acids present in the matrix and the subsequent anhydride formation; decarboxylation of the remaining unsaturated carboxylic acids; and formation of amides (out of non-coordinated ammonium carboxylates) and their evaporation.

The TGA-MS profile of m/q 18 in Fig. 4 clearly indicates the drying of the precursor gel between room temperature and 140 °C.

From 100 °C on, with a maximum near 160 °C, the evolution of NH_3 is detected in TGA-MS. The matching appearance of carboxylic acids in the HT-DRIFT spectrum ($\nu(C=O)_{COOH}$ at 1720 cm^{-1} in Fig. 3) at these temperatures indicates the decomposition of the ammonium carboxylate structure of the gel, as previously shown for other aqueous precursor gels [6, 7].

The detection of m/q 60 in TGA-MS at low temperatures (between 160 °C and 260 °C), corresponding with the molecular ion of acetic acid, and the accompanying evolution of NH_3 is indicative [6, 7] for the decomposition (and former presence) of ammonium acetates in the PZT gel.

The dehydroxylation of α-hydroxy-carboxylates/α-hydroxy-carboxylic acids towards unsaturated carboxylates/carboxylic acids and the subsequent anhydride formation can be confirmed by the detection of water

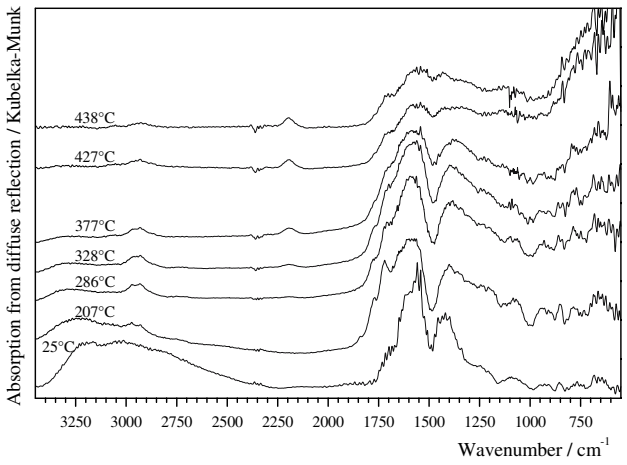

Fig. 3 HT-DRIFT spectra for the decomposing PZT precursor gel in dry air at a heating rate of 10 °C min^{-1}

(m/q 18) in TGA-MS around 210 °C and the typical absorption of anhydrides at 1850 cm^{-1} and 1780 cm^{-1} in the HT-DRIFT spectrum at 207 °C (caused by the cyclic itaconic and citraconic anhydride) [7].

The decarboxylation of the remaining unsaturated carboxylic acids is confirmed by the evolution of CO_2 (m/q 44) at 220 °C and the slow disappearance of the carboxylic acid carbonyl stretch $\nu(C=O)_{COOH}$ at 1720 cm^{-1} in the HT-DRIFT spectra at more elevated temperatures (e.g. in the spectrum at 286 °C).

The formation of amides (out of ammonium carboxylates) and their evaporation can be confirmed by the detection of m/q 59 in TGA-MS, since m/q 59 refers to $(H_2N)(HO)C=CH_2^+$, a typical ion fragment formed by a McLafferty rearrangement after ionization of an amide containing a γ-H [32,33].

In the second temperature region (from 270 °C until 420 °C) the direct coordination of the metal ions does change. The DTA profile between 270 °C and 330 °C in Fig. 2 gives evidence for an endothermal reaction that probably corresponds with the breakdown of the α-hydroxy-coordination of the metal ion. This statement is strengthened by the disappearing absorption of the ν(C-O) stretch at 1090 cm^{-1} in the HT-DRIFT spectra of the same temperature interval (compare the spectra of 286 ° and 336 ° with the one of 207 °C in Fig. 3). The temperature at which the breakdown of the α-hydroxy-coordination occurs is representative for most other aqueous metal citrate precursor complexes [6, 7].

At slightly higher temperature, between 340 °C and 420 °C, a second evolution of m/q 44 is detected in TGA-MS. The exothermal evolution of CO_2 can typically be attributed to the ongoing decomposition of the metal ion carboxylates once the coordination of the α-hydroxy-group has disappeared [7] : the corresponding HT-DRIFT spectra at 377 °C and 420 °C show a decreased absorption intensity for metal carboxylate stretches ($\nu_{as}(COO^-/M^{z+})$ and $\nu_{sym}(COO^-/M^{z+})$) when compared with the spectrum at 328 °C (at 1575 cm^{-1} and 1395 cm^{-1} respectively). Since the ammonium carboxylate bonds have already been expelled at lower temperature the decreasing IR absorption in this energy region can only be attributed to the decomposition of metal carboxylate bonds.

From the HT-DRIFT spectra of Fig. 3 it is not directly apparent at what temperature the side-on peroxo-groups are decomposed. Although one can clearly distinguish the $\nu_1(M<O_2)$ stretch at 850 cm^{-1} in the HT-DRIFT spectrum of 286 °C, it is difficult to resolve its presence at higher temperatures because of the increased absorbance of metal oxygen stretches ν(M-O) in the fingerprint region. Given the spectra of Fig. 3, the peroxo-groups probably remain coordinated to the metal ions during the entire second temperature region.

In the second temperature region the remaining organic compounds are decomposed as well: the absorbance at 2200 cm^{-1} in the HT-DRIFT-spectra of Fig. 3 clearly indicates the formation and presence of nitrilles at 328°C and higher temperatures. Moreover, in TGA-MS one can unmistakably detect m/q 41, that gives good evidence for the evolution of aliphatic nitrilles, since this m/q is a archetypal ion fragment for nitrilles with a γ-H (the $HN=C=CH_2^+$-ion is typically formed through a McLafferty rearrangement after ionization) [32,33].

In the third temperature region (from 420 °C until 520 °C) the residual organic matrix is decomposed oxidatively and metal oxide bonds are formed. The rapid weight loss and the highly exothermal nature of the decomposition at 435 °C, as shown in Fig. 2, indicate a sudden ignition and oxidative combustion of the organic residue. This statement is supported by the fact that the oxygen pressure in the TGA-furnace, and therefore as well in the MS apparatus, drops suddenly at this temperature, as illustrated in Fig. 4.

Because of this fast combustion at lower oxygen pressure not only CO_2 (m/q 44), water (m/q 18) and NO (m/q 30) are detected, but also evolving nitrilles (m/q 41) and ammonia (m/q 17) are distinguished at 435 °C: the oxidation at this temperature is therefore incomplete. The HT-DRIFT spectra at 427 °C and 438 °C in Fig. 3 confirm the combustion of organic matter, given that the total absorbance of the corresponding functional groups decreases drastically in between 2000 cm^{-1} and 1000 cm^{-1} (e.g. the carbonyl and the carboxylate stretches). The extensive formation

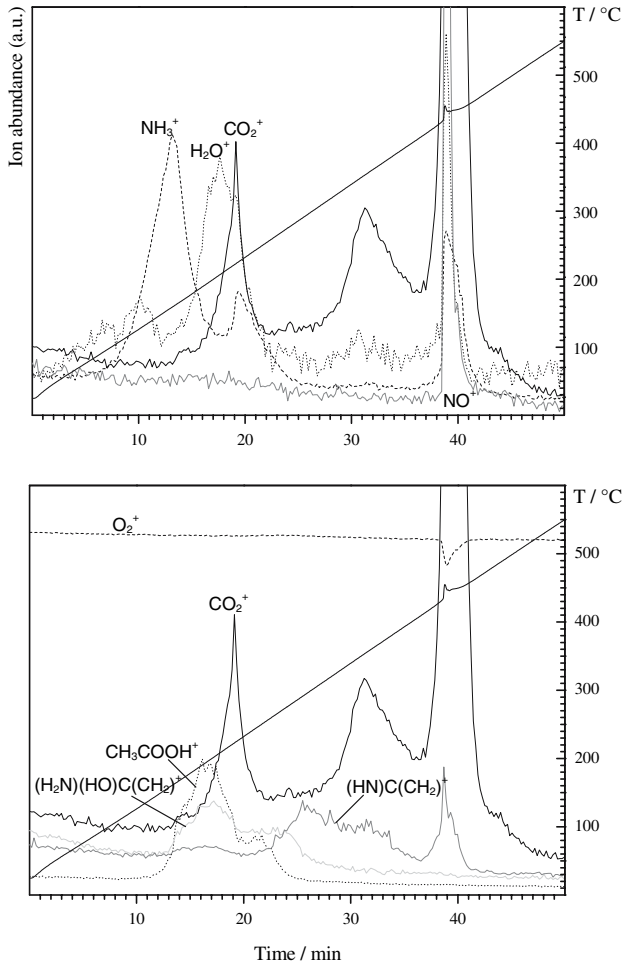

Fig. 4 Abundances of ion fragments (m/q) detected in TGA-MS for the decomposing PZT precursor gel heated at 10 °C min^{-1} in dry air. Upper: m/q 44 (solid—CO_2^+); m/q 17 (dash—NH_3^+); m/q 18 (dot—H_2O^+); m/q 30 (NO^+—dark grey solid). Lower: m/q 44 (solid—CO_2^+); m/q 32 (dash—O_2^+); m/q 60 (dot—CH_3COOH^+); m/q 41 (dark grey solid—$(HN)C(CH_2)^+$); m/q 59 (light grey solid—$(H_2N)(HO)C(CH_2)^+$)

of metal-oxygen bonds, and hence the onset of oxide formation, can be deduced from the increased total absorbance in the ν(M-O) region (below 900 cm^{-1}).

The tail of the DTG curve and the final minor release of CO_2, observed at the end of the m/q 44 abundance profile in TGA-MS, indicate an ongoing slower decomposition of the organic matter until 520 °C, where after the absolute mass remains constant and the pyrolysis of the precursor is considered complete.

When compared with the decomposition of other (multi)metal oxides prepared through aqueous solution-gel chemistry [2, 6, 7], it is clear that the thermal disintegration of the PZT gel is typical and can roughly be described by three successive events: the endothermal decomposition of the non-coordinative matrix surrounding the metal ion complexes, the disintegration of the precursor complexes and the combustion of the remaining organic matrix.

Phase formation of perovskite PZT

Beside the study of the thermal decomposition of the PZT gel structure, the phase formation of crystalline oxides during the thermal treatment of the precursor is investigated in situ as well. In Fig. 5 the HT-XRD patterns for a bulk stoichiometrical PZT precursor

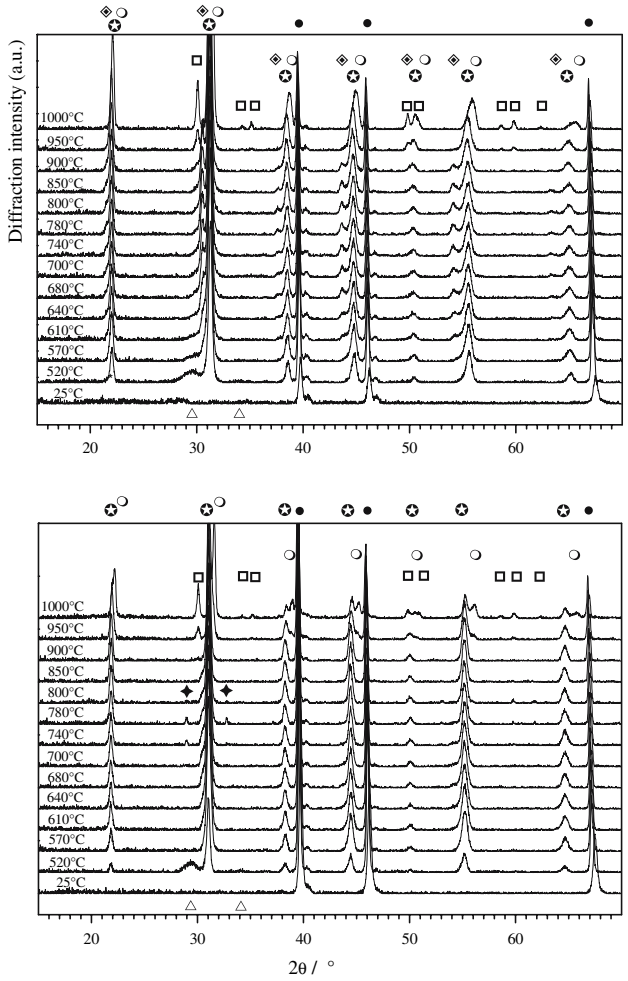

Fig. 5 Upper: HT-XRD spectra of the stoichiometrical PZT gel heated at 10 °C min^{-1} in static dry air. The following crystalline phases were attributed: ✪ *Pe* PZT (MPB); △ *Py* PZT; ● Pt; ❍ *Pe* $PbTiO_3$; ◈ *Pe* $PbZrO_3$; and □ ZrO_2 or $Zr_{1-x}Ti_xO_2$. The reflections at 39.76°, 46.24° and 67.45° 2θ are originating from the Pt sample holder. Lower : HT-XRD spectra of a PZT gel containing a 16 mol% excess of lead, heated at 10 °C min^{-1} in static dry air. The following crystalline phases were attributed: ✪*Pe* PZT (MPB); △ *Py* PZT; ● Pt; ❍ *Pe* $PbTiO_3$; □ ZrO_2 or $Zr_{1-x}Ti_xO_2$; and ✦PbO (massicot)

without excess lead are shown (for a heating rate of 10 °C min^{-1} in static dry air).

Directly after the full decomposition of the organics in the gel (at 520 °C) the amorphous precursor turns into a mixture of crystalline pyrochlore (*Py*) and perovskite (*Pe*) PZT (JCPDS – database no.33-0784) [34]. While the *Pe* PZT phase is clearly abundant, the *Py* PZT phase only shows weak and broad reflections at this temperature. Moreover the minor fraction *Py* PZT does not seem to be stabile and converts rather quickly into crystalline *Pe* PZT above this temperature: at 610 °C no *Py* PZT is detected anymore.

At higher temperature phase segregation occurs: at 610 °C one can clearly identify the presence of a zirconium rich *Pe* PZT phase; the Bragg reflections of this phase bear strong resemblance to that of $PbZrO_3$ (JCPDS – database no.35-0739). This zirconium rich PZT phase further crystallizes at higher temperature, until it diminishes from 950 °C on.

At very high temperatures (950 °C/1000 °C) a Ti-rich PZT phase is formed, its diffraction spectrum resembles that of $PbTiO_3$ (JCPDS – database no.40-0099). The segregation of this phase coincides with the formation of $Zr_{1-x}Ti_xO_2$ and/or ZrO_2 (JCPDS – database no.42-1164) in the sample.

The existence of these segregated phases might be linked to the endothermal reaction corresponding with the (0.5 w%) weight loss at elevated temperatures, shown in Fig. 2. Since, both these phenomena have been attributed earlier to the sublimation of lead(II)-oxide (PbO) [4], it is most probable that the occurring segregations are caused by the non-stoichiometry of the multimetal oxide at elevated temperatures (the multimetal oxide becomes lead short during heating). Therefore the PZT precursor sample with a 16 mol% excess of lead was submitted to the same HT-XRD experiment. It is known for these typical compositions that destructive PbO-loss, leading to lead deficiencies, can be avoided and better ferroelectric properties can be obtained [35–38]. The excess lead balances the loss due to sublimation, leading to better ferroelectric properties.

Figure 5 shows the HT-XRD patterns of the lead rich PZT precursor. Similar to the previous precursor a mixture of *Pe* and *Py* PZT crystallizes from the amorphous sample at 520 °C; the *Py* PZT then rapidly converts to *Pe* PZT above this temperature. At higher temperatures the segregation of a zirconium rich PZT phase is no longer observed: only *Pe* PZT is detected up to 740 °C. This observation clearly confirms the accredited role of the excess lead used in the PZT synthesis.

At 740 °C, the remaining excess of lead crystallizes under the form of PbO (massicot), which remains present up to 800 °C. At higher temperatures the sublimation (and evaporation) of PbO proceeds nonetheless: once again the formation of a Ti-rich PZT phase, $Zr_{1-x}Ti_xO_2$ and ZrO_2 occurs at 950 °C/1000 °C.

Conclusions

Starting form a novel water-based Zr(IV)-peroxo-citrato precursor solution, an entirely aqueous solution-gel synthesis of $Pb(Zr_{0.53},Ti_{0.47})O_3$ (PZT) could be carried out.

Therefore the, as such insoluble, Zr^{4+} ion had to be chemically modified to a water-soluble peroxo-citrato complex. By evaporating water from an aqueous solution containing Zr(IV)-peroxo-citrato-, Ti(IV)-peroxo-citrato- and Pb(II)-citrate complexes, a transparent amorphous PZT gel precursor was obtained. The gel structure consists of a network of cross-linked ammonium-carboxylate bonds wherein all metal ion complexes are intimately mixed.

By combining several (complementary) thermal analysis techniques the thermal decomposition mechanism of the aqueous PZT gel was unraveled. In the decomposition pathway three major temperature regions could be distinguished, wherein consecutively the disintegration of the non-coordinative matrix surrounding the metal ion complexes, the precursor complexes, and the remaining organic matrix are observed.

The phase formation study of crystalline perovskite PZT showed that sublimation of PbO leads to phase segregation of a Zr-rich PZT phase for a stoichiometrical PZT precursor. However single phase perovskite PZT could be obtained at low temperature (610 °C) when a typical 16% lead excess was applied.

Further work will be focused on the chemical solution deposition (CSD) of thin ferroelectric PZT films and their properties. Given that it is now possible to obtain *Pe* PZT from aqueous solution-gel chemistry at low temperatures and the fact that deposition of thin aqueous layers on top of appropriate substrates is no longer a problem [9–12], one is encouraged to investigate the CSD of PZT by means of the aqueous solution-gel method [14].

Acknowledgements K. Van Werde is indebted to the 'Instituut voor de aanmoediging van Innovatie door Wetenschap en Technologie in Vlaanderen' (I.W.T. – Flanders - Belgium) for financial support. G. Vanhoyland and M. K. Van Bael are post doctoral fellows of the Fund for Scientific Research Flanders, Belgium (F.W.O.-Vlaanderen).

References

1. Narendar Y, Messing GL (1997) Catal Today 35:247
2. Narendar Y, Messing GL (1997) Chem Mater 9:580
3. Nelis D, Van Werde K, Mondelaers D, Vanhoyland G, Van Den Rul H, Van Bael MK, Mullens J, Van Poucke LC (2003) J Sol-Gel Sci Technol 26:1125
4. Van Werde K, Vanhoyland G, Nelis D, Mondelaers D, Van Bael MK, Mullens J, Van Poucke LC (2001) J Mater Chem 11:1192
5. Mullens J, Van Werde K, Vanhoyland G, Nouwen R, Van Bael MK, Van Poucke LC (2002) Thermochim Acta 392–393:29
6. Hardy A, Van Werde K, Vanhoyland G, Van Bael MK, Mullens J, Van Poucke LC (2003) Thermochim Acta 397:143
7. Van Werde K, Mondelaers D, Vanhoyland G, Nelis D, Van Bael MK, Mullens J, Van Poucke LC, Van Der Veken B, Desseyn HO (2002) J Mater Sci 37:81
8. Kareiva A, Tautkus S, Rapalaviciute R, Jorgensen J-E, Lundtoft B (1999) J Mater Sci 34:4853
9. Zanetti SM, Longo E, Leite ER, Varela JA (1999) J Eur Ceram Soc 19:1409
10. Mondelaers D, Vanhoyland G, Van Den Rul H, D'haen J, Van Bael MK, Mullens J, Van Poucke LC (2003) J Sol-Gel Sci Technol 26:523
11. Nelis D, Van Bael MK, Van Den Rul H, Mullens J, Van Poucke LC, Vanhoyland G, D'haen J, Laureyn W, Wouters DJ (2002) Integr Ferroelectrics 45:205
12. Van Bael MK, Nelis D, Hardy A, Mondelaers D, Van Werde K, D'haen J, Vanhoyland G, Van Den Rul H, Mullens J, Van Poucke LC, Frederix F, Wouters DJ (2002) Integr Ferroelectrics 45:113
13. Nelis D, Van Werde K, Mondelaers D, Vanhoyland G, Van Bael MK, Mullens J, Van Poucke LC (2001) J Eur Ceram Soc 21:2047
14. Van Genechten D, Vanhoyland G, D'haen J, Wouters DJ, Vanhoutem I, Van Bael MK, Van Den Rul H, Mullens J, Van Poucke LC, To be published
15. Moulson AJ, Herbert JM (1990) Electroceramics: Materials, Properties And Applications. Chapman & Hall, Londen
16. Schwartz RW, Schneller T, Waser R (2004) CR Chimie 7:433, and references within
17. Richens DT (1997) The Chemistry Of Aqua Ions; Synthesis, Structure And Reactivity. John Wiley & Sons, Chichester
18. Malic B, Kosec M, Smolej K, Stavber S (1999) J Eur Ceram Soc 19:1345
19. S Hoffmann R Waser (1999) J Eur Ceram Soc 19:1339
20. Mullens J (1998) In: Gallagher PK, Brown ME (eds) Handbook of thermal analysis and calorimetry: Vol. I: Principles and practice – Chapter 12: Evolved gas analysis. Elsevier, Amsterdam, p 509
21. ''Thermolab Instruction manual: evolved gas analyser for thermal analysis – mass spectrometry'' (Fisons Instruments), p 37
22. Livage J, Henry M, Sanchez C (1988) Prog Solid St Chem 18:259
23. Jolivet JP, Henry M, Livage J (2000) Metal Oxide Chemistry And Synthesis : From Solution To Solid State. Wiley, Chichester
24. Kakihana M (1996) J Sol-Gel Sci Technol 6:7
25. Van Bael MK, Arčon I, Van Werde K, Nelis D, Mullens J, Van Poucke LC (2005) Physica scripta T115:415
26. Djordjevic C, Lee M, Sinn E (1989) Inorg Chem 28 :719
27. Thompson RC (1985) Inorg Chem 25:3542
28. Soares MR, Senos AMR, Mantas PQ (1999) J Eur Ceram Soc 19:1865
29. Dengel AC, Griffith WP (1989) Polyhedron 8:1371
30. Schwartz RW (1997) Chem Mater 9:1
31. Van Genechten D, Vanhoyland G, D'haen J, Johnson J, Wouters DJ, Van Bael MK, Van Den Rul H, Mullens J, Van Poucke LC (2004) Thin Solid Films 467:104
32. Sorrell TN (1988) Interpreting spectra of organic molecules. University Science Books, Mill Valley
33. Lee TA (1998) A beginners guide to mass spectral interpretation. Wiley, Chichester
34. Jcpds –International Centre For Diffraction Data, 1997
35. Nouwen R, Mullens J, Franco D, Yperman J, Van Poucke LC (1996) Vibrational Spectroscopy 10:291
36. Lefevre MJ, Speck JS, Schwartz RW, Dimos D, Lockwood SJ (1996) J Mater Res 11:2076
37. Wang ZJ, Kikuchi K, Maeda R (2000) Jpn J Appl Phys Part I 39(9b):5413
38. Burmistrova PV, Sigov AS, Vasiliev AL (2002) Ferroelectrics 271:1641